Supporting information:

Organic/inorganic self-doping controlled crystallization and electronic properties in mixed perovskite solar cells

Tongle Bu[a], Xueping Liu[a], Rui Chen[a], Ziwen Liu[a], Kunpeng Li[a], Wangnan Li[b], Zhiliang Ku[a], Yong Peng[a], Fuzhi Huang[a], Yi-Bing Cheng[a,c] and Jie Zhong[a]*

[a]State Key Laboratory of Advanced Technology for Materials Synthesis and Processing, Wuhan University of Technology, Wuhan 430070, P. R. China

[b]Hubei Key Laboratory of Low Dimensional Optoelectronic Materials and Devices, Hubei University of Arts and Science, Xiangyang 441053, P. R. China

[c]Department of Materials Science and Engineering, Monash University, VIC 3800, Australia

*Corresponding Email: jie.zhong@whut.edu.cn;

Experimental section

Materials

Unless specified, otherwise all chemicals were purchased from Aladdin, Alfa Aesar or Sigma-Aldrich and used as received. 30NR titanium oxide (TiO_2) paste was purchased from Dyesol. Formamidinium iodide (FAI), methylammonium bromine (MABr), and lead bromine ($PbBr_2$) were purchased from Lumtec, Taiwan. Lead iodide (PbI_2) was purchased from TCI. Spiro-OMeTAD was purchased from Xi'an Polymer Light Technology Corp.

Preparation of the self-doping mixed perovskite precursors

The self-doping mixed perovskite precursors were prepared by composed two parts, one part is the organic precursors composed of 0.85 FAI and 0.15 MABr, and the other part is the inorganic precursors composed of 0.85 PbI_2 and 0.15 $PbBr_2$. Both of the two parts were dissolved in a co-solvent of DMF/DMSO (4:1, by volume) according to a ratio of R value (R=organic precursor/inorganic precursor) changed from 0.35 to 1.75. And the concentration of perovskite precursors was controlled to 1.3M.

Device fabrication

FTO glass was etched by a laser machine (Universal Laser Systems, VLS2.30), followed by ultrasonic cleaning through detergent, pure water and ethyl alcohol for 20 min, respectively. They were then dried with dry-air gas flow and finally treated under oxygen plasma for 10 min to remove the last traces of organic residues. The compact TiO_2 blocking layer was first deposited on the clean FTO glass at 450 °C by the pyrolysis of isopropanol diluted Titanium diisopropoxide (bis-2,4-

pentanedionate) (1:10 by volume), and then cooled to room temperature. Then a thickness of 150 nm~200 nm TiO_2 mesoporous layer was prepared by spun of ethanol and terpinol diluted 30NR paste (1:1:4 by weight), at 4000 rpm for 30 s, followed by annealing at 120 °C for 10 min and then sintering at 500 °C for 30 min with a ramp time of 1 hour. After cooling down, a 20μL of 0.1 M Li-TFSI which was dissolved in acetonitrile was spun on the mesoporous TiO_2 substrate at 4000 rpm for 30 s and annealed at 450°C for another 30 min. The different perovskite layers were deposited by spun a 25 μL mixed perovskite precursor solution at 6000 rpm for 30 s with an accelerated speed of 1000 rpm, and a 100 μL chlorobenzene was dropped at the last 5th second. The films were then annealed at 100 °C for an hour, and after cooling down, a 25 μL spiro-OMeTAD solution was spun on the film at 3000 rpm for 30 s which prepared by dissolving 83.2 mg spiro-OMeTAD, 15.8 μL of a stock solution of 500 mg lithium bis(trifluoromethylsulphonyl)imide in 1 mL acetonitrile and 34 μL 4-tert-butylpyridine in 1 mL chlorobenzene. At last a 60 nm of gold was evaporated as the back electrode to form the whole devices.

Characterizations

The surface morphologies and microstructures of the perovskite films and cross-sectional structure of the perovskite solar cells were investigated using a field-emission scanning electron microscopy (FESEM, Zeiss Ultra Plus). The different self-doping perovskite films were tested by an X-ray diffractometer (XRD, D8 Advance), UV-vis (lambda 750S, PerkinElmer), fourier transform infrared spectroscopy (FTIR, VERTEX 70, Bruker, Germany), atomic force microscope (AFM, SPM9700, Shimadzu, Japan) and the surface chemical state of different self-doping perovskite films was investigated using an X-ray photoelectron spectroscopy (XPS, Thermo Scientific K-Alpha). The time-resolved photoluminescence (TRPL) was measured at 770 nm using excitation with a 478nm light pulse from Delta Flex Fluorescence Lifetime System (Horiba Scientific Com., Japan)**.** The EIS measurements were carried out by a EC-lab (SP300). The photocurrent density-voltage curves of the perovskite solar cells were measured using a solar simulator (Oriel 94023A, 300 W) and a Keithley 2400 source meter. The intensity (100 mW/cm^2) was calibrated using a standard Si solar cell (Oriel, VLSI standards). All the devices were tested under AM 1.5G sun light (100 mW/cm^2) using a metal mask of 0.16 cm^2 (except the big size devices) with a scan rate of 10 mV/s.

Table S1. Surface roughness of different self-doping perovskite films.

Ratio (R)	0.35	0.56	0.75	0.93	1.00	1.08	1.17	1.4	1.75
Ra (nm)	172	26.33	25.64	25.41	25.27	25.15	25.17	28.14	40

Table S2. Surface elements content of R=0.93, R=1.00 and R=1.08 perovskite films.

Atomic %	**R=0.93**	**R=1.00**	**R=1.08**
C	57.1	43.1	42.1
Pb	11.0	13.4	14.1
I	30.8	43.0	42.4
Br	1.1	1.2	1.4

N	<.1	<.1	<.1

Table S3. Average and champion photovoltaic parameters derived from *J-V* measurements of different perovskite based devices.

R	*Voc* （V)	*Jsc* (mA/cm^2)	FF	PCE （%）
0.35	0.611±0.033	0.22±0.06	0.50±0.05	0.07±0.02
	0.602	**0.31**	**0.58**	**0.11**
0.56	1.043±0.031	2.62±0.34	0.62±0.03	1.71±0.26
	1.051	**3.01**	**0.64**	**2.02**
0.70	1.066±0.027	6.01±0.24	0.65±0.02	4.17±0.20
	1.084	**6.25**	**0.65**	**4.39**
0.93	1.079±0.019	15.93±0.61	0.67±0.03	11.55±0.66
	1.091	**15.94**	**0.70**	**12.12**
1.00	1.056±0.011	21.79±0.60	0.71±0.02	16.33±0.55
	1.085	**22.12**	**0.73**	**17.51**
1.08	1.092±0.015	22.23±0.66	0.73±0.02	17.72±0.59
	1.125	**22.63**	**0.75**	**19.14**
1.17	1.092±0.019	19.51±0.76	0.68±0.02	14.42±0.38
	1.117	**19.48**	**0.68**	**14.79**
1.40	1.103±0.015	18.27±0.81	0.67±0.02	13.61±0.48
	1.119	**18.29**	**0.69**	**14.21**
1.75	0.929±0.051	12.19±0.95	0.49±0.04	5.57±0.50
	0.972	**12.55**	**0.48**	**5.82**

Table S4. Comparison of PL decay fitting parameters between different self-doping perovskite films.

R	τ_1 (ns)	τ_2 (ns)
0.35	4.84	75.1
0.56	6.64	140
0.70	17.4	121
0.93	35.6	930
1.00	33.3	986
1.08	72.1	1110
1.17	69.2	618
1.40	67.8	274
1.75	65.6	269

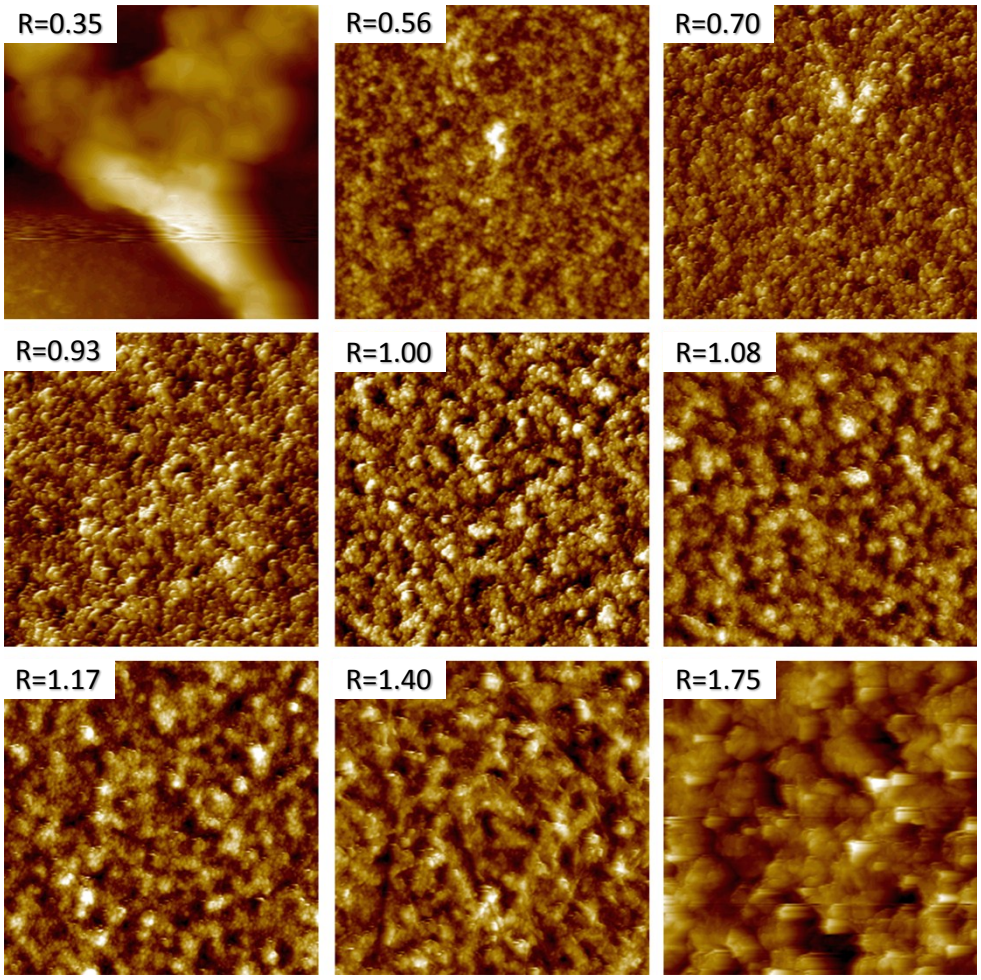

Fig S1. Surface AFM images of different self-doping perovskite films. The selected scan area is 20×20 μm.

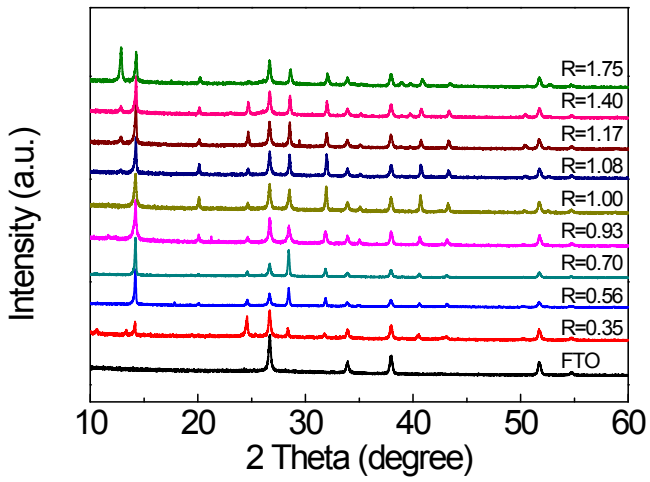

Fig S2. XRD pattern of different self-doping perovskite films.

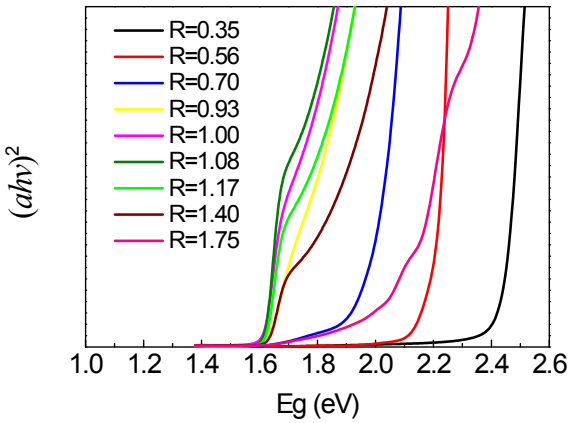

Fig S3. The bandgap of different self-doping perovskite films.

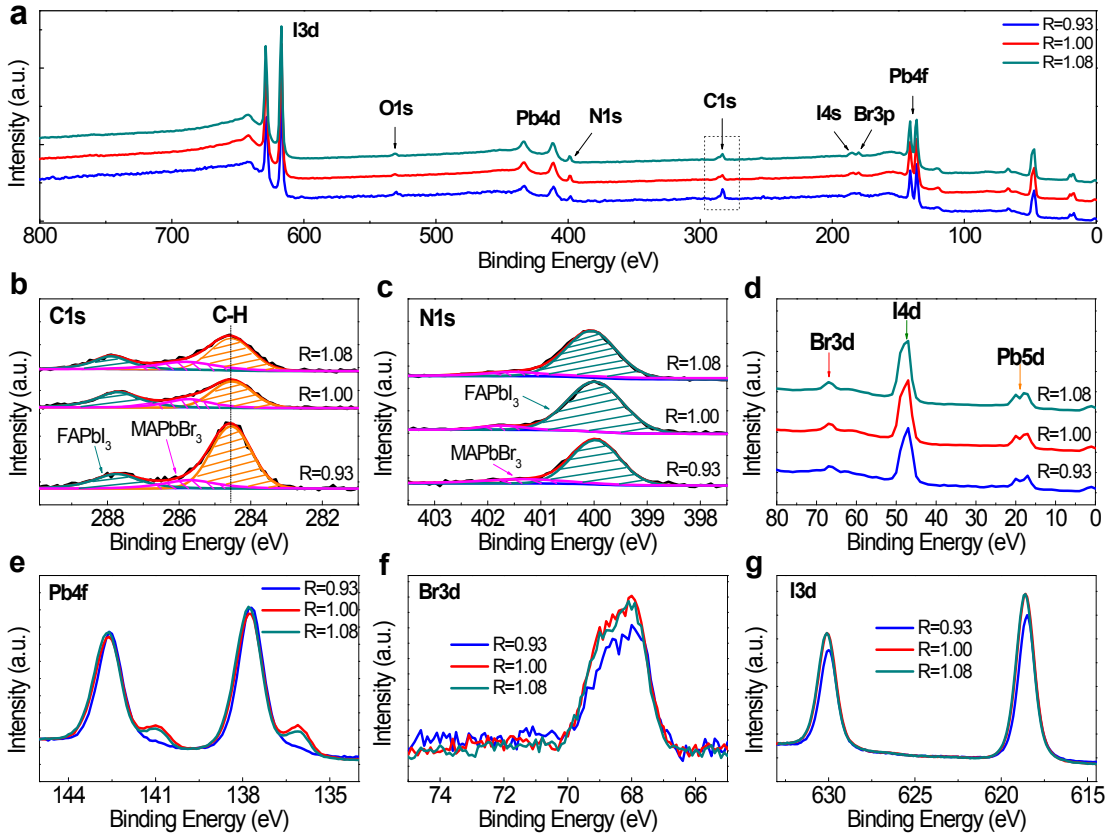

Fig S4. (a) XPS overview spectra, (b) C1s core level, (c) N1s core level, (d) Br3d/I4d/Pb5d, (e) Pb4f, (f) Br3d and (g) I3d core level peaks spectra of R=0.93, R=1.00 and R=1.08 perovskite films, respectively.

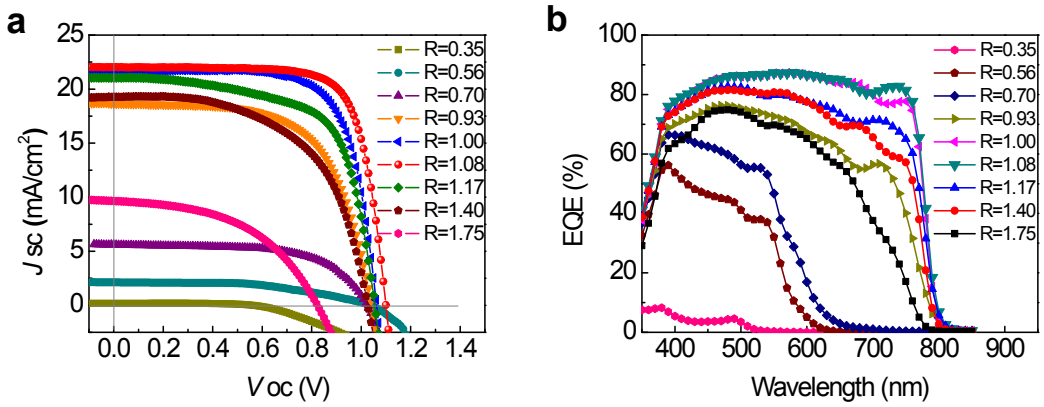

Fig S5. (a) *J-V* curves of different self-doping perovskite devices, and (b) the corresponding EQE spectra.

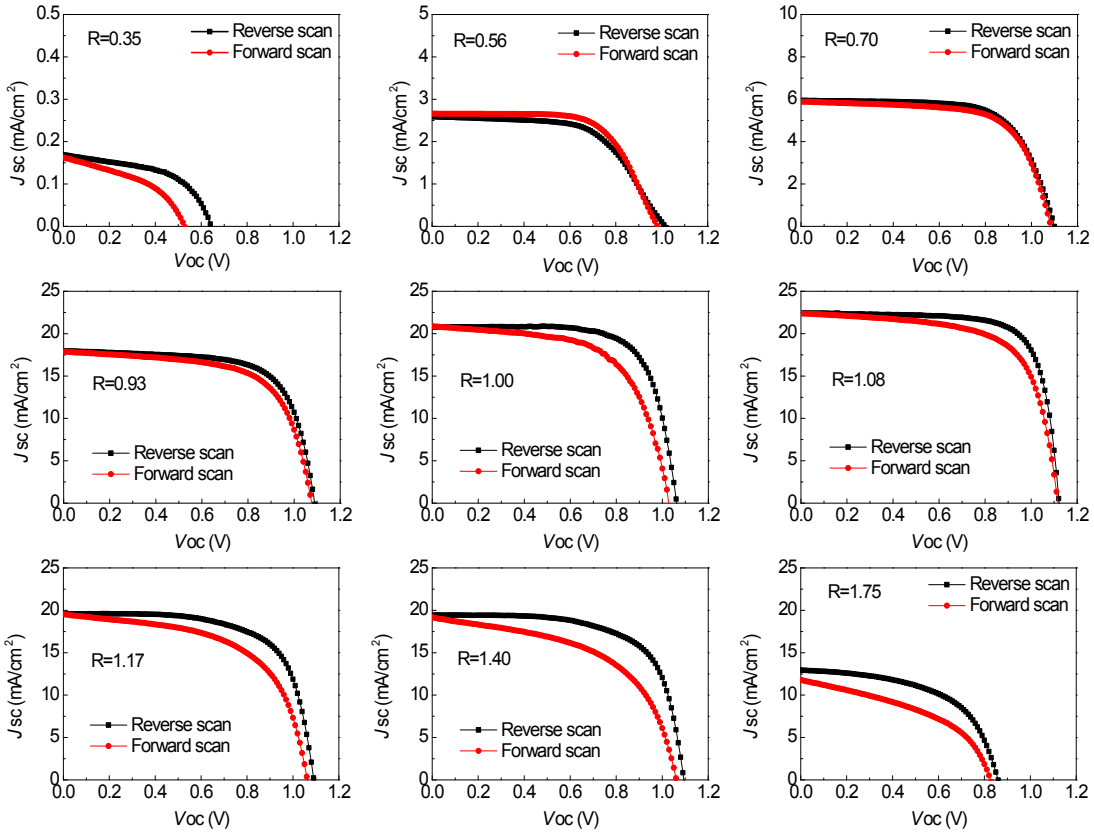

Fig S6. Typical *J-V* curves of reverse scan and forward scan for different self-doping perovskite devices.

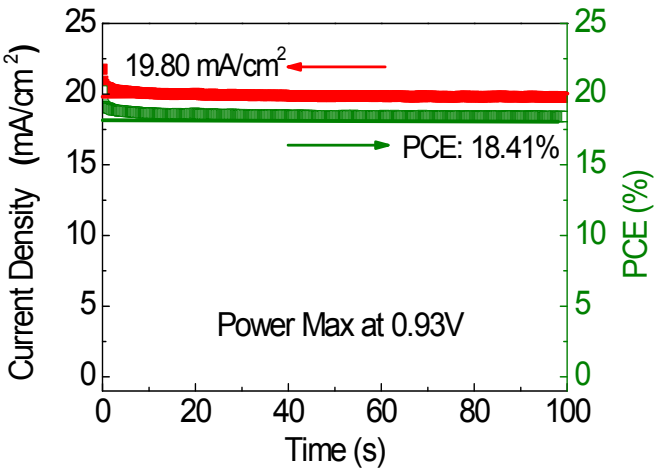

Figure S7. Stable photocurrent density and PCE measured at 0.93 V forward bias, the cell was in the light under open-circuit prior to the start of the measurement.

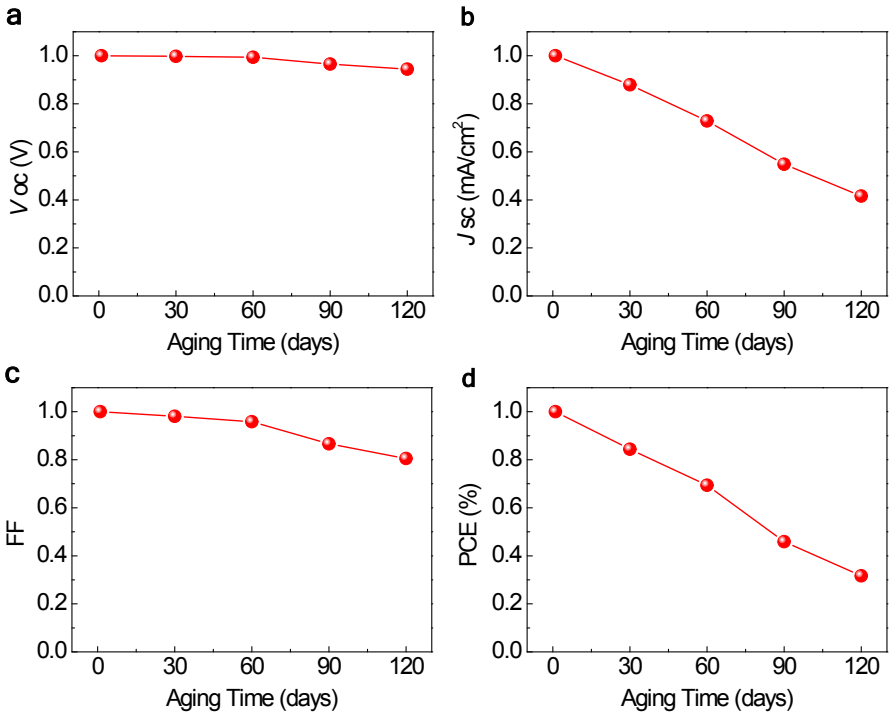

Fig. S8 Stability test of R=1.08 perovskite solar cells with big area up to1.21cm^2 under ambient environment (>60 RH%). Normalized (a) V_{oc}, (b) J_{sc}, (c) FF and (d) PCE versus aging time curves, respectively.